Interaction of Oscillations, and Their Suppression via Deep Brain Stimulation, in a Model of the Cortico-Basal Ganglia Network

Guiyeom Kang and Madeleine M. Lowery, *Member, IEEE*

***Abstract*—Growing evidence suggests that synchronized neural oscillations in the cortico-basal ganglia network may play a critical role in the pathophysiology of Parkinson's disease. In this study, a new model of the closed loop network is used to explore the generation and interaction of network oscillations and their suppression through deep brain stimulation (DBS). Under simulated dopamine depletion conditions, increased gain through the hyperdirect pathway resulted in the interaction of neural oscillations at different frequencies in the cortex and subthalamic nucleus (STN), leading to the emergence of synchronized oscillations at a new intermediate frequency. Further increases in synaptic gain resulted in the cortex driving synchronous oscillatory activity throughout the network. When DBS was added to the model a progressive reduction in STN power at the tremor and beta frequencies was observed as the frequency of stimulation was increased, with resonance effects occurring for low frequency DBS (<40 Hz) in agreement with experimental observations. The results provide new insights into the mechanisms by which synchronous oscillations can arise within the network and how DBS may suppress unwanted oscillatory activity.**

***Index Terms*—Basal ganglia, deep brain stimulation (DBS), oscillations, Parkinson's disease.**

I. Introduction

OVER the past decade, deep brain stimulation (DBS) has become established as an effective therapy for treating the symptoms of Parkinson's disease including tremor, bradykinesia, rigidity, and akinesia. Recent studies have suggested that DBS disrupts abnormal neural synchrony responsible for pathological oscillations throughout the cortico-basal ganglia network [1], [2]. In patients with Parkinson's disease and MPTP-treated monkeys, increased oscillatory activity in the local field potential (LFP) and synchronized neural activity within the parkinsonian tremor (3–9 Hz) and beta (15–45 Hz) frequency ranges have been shown to occur throughout the basal ganglia, including the subthalamic nucleus (STN), globus pallidus externa (GPe), and interna (GPi), and in the cortex [3]–[6]. LFP and surface electromyographic signals have been shown to be correlated both at the frequency, and at twice the frequency, of parkinsonian tremor [7], [8]. Recently, directional coupling between LFP and accelerometer signals has confirmed an efferent role for LFP oscillations in the generation of tremor [9]. The strength of beta band oscillations and levels of bradykinesia and rigidity are correlated in Parkinson's disease, and are suppressed with the degree of suppression inversely correlated to symptom severity following administration of Levodopa [10]–[12]. Beta band power in the STN is similarly attenuated during and following STN-DBS [13]–[15], leading to the hypothesis that DBS may exert part of its therapeutic influence through the suppression of pathological beta band activity.

Two main hypotheses have been proposed to explain the origin of the pathological oscillations in Parkinson's disease. The first, based on *in vitro* recordings from STN-GPe network co-cultured with the cortex and striatum suggests that low-frequency oscillatory activity is generated by the reciprocally connected STN-GPe network acting as a central pacemaker [16]. Dopamine depletion presynaptically increases the effect of GABAergic transmission from the GPe to STN, contributing to abnormal correlated burst-firing among STN neurons [17]. These effects are further enhanced by decreased activation of postsynaptic dopamine receptors in the STN [18]. It has been alternatively suggested that dopaminergic loss leads to a loss of segregation among nuclei within the cortico-basal ganglia network, leading to increased synchrony and oscillatory activity throughout the network [19].

Recent studies have suggested a critical role for overactivity in the hyperdirect pathway between the cortex and STN in the generation of pathological oscillations in Parkinson's disease [20]. It has been shown that abnormal slow oscillations of the STN-GPe network can be driven by the cortex following dopamine depletion [20]–[22]. It is possible that a similar mechanism may underpin exaggerated beta activity in the cortex and STN, with the cortex effectively driving the STN in Parkinson's disease. Consistent with this, measures of functional connectivity in animal models of Parkinson's disease have indicated increased coupling between the cortex and STN and between the STN and GPe [21]–[24]. It is also possible that oscillations originating in different parts of the network may interact leading to loss of segregation at the network level. Bispectral analysis has provided experimental evidence of nonlinear interactions between different basal ganglia oscillations in Parkinson's disease patients that can be modulated by administration of Levodopa [25], [26]. Despite these advances, current understanding of the origin and functional significance

Manuscript received April 25, 2012; revised November 07, 2012; accepted December 23, 2012. Date of current version March 07, 2013. This work was supported in part by the Irish Research Council for Science, Engineering and Technology under Grant RS/2009/1330 and in part by the Science Foundation Ireland under Grant 05/RF/ENM047.

The authors are with School of Electrical, Electronic and Communications Engineering, University College Dublin, Ireland (e-mail: guiyeom.kang@ucd.ie; madeleine.lowery@ucd.ie).

Digital Object Identifier 10.1109/TNSRE.2013.2241791

of pathological oscillatory activity within the cortico-basal ganglia network and the mechanism by which they are modulated by DBS is far from complete.

In this study, we explore the hypothesis that alteration in network connectivity due to dopamine depletion in Parkinson's disease leads to the generation of pathological oscillations within the cortico-basal ganglia network and that high-frequency DBS exerts its therapeutic influence by suppressing these oscillations, using model simulation. We explore mechanisms by which low frequency oscillations can be generated within the network and illustrate how oscillations at both beta and tremor frequencies can emerge through the interaction of oscillatory STN activity with cortical inputs through the hyperdirect pathway.

The model presented is the first to simulate activity of individual neurons in each of the nuclei in the closed loop formed through the cortico-basal ganglia-thalamic network. The model also simulates pathological oscillations at both beta and parkinsonian tremor frequencies. The majority of DBS models to date have focused on the network formed by the STN, GPe, GPi, and thalamus without consideration of cortical inputs and have simulated pathological oscillations at the frequency of parkinsonian tremor [27]–[31]. The effect of DBS on simulated beta oscillations was examined in [32], however the model did not consider oscillations at the frequency of parkinsonian tremor nor the closed loop formed between the cortex and basal ganglia. While these nuclei have been included in a recent neural mass model [33], by its nature this type of model focuses on the aggregate activity of populations of neurons, and therefore does not capture individual neuron firing times and dynamics.

In this paper, we illustrate how under conditions of increased gain through the hyperdirect pathway neural oscillations at two different frequencies arising within the cortex and STN can interact, leading to the emergence of synchronized oscillations throughout the network at a new intermediate frequency. The model also shows how cortical activity may dominate and drive the activity of the STN at higher gains. In agreement with experimental observations, the addition of high frequency DBS to the model suppressed oscillations in the STN at both parkinsonian tremor and beta frequencies, while low frequency DBS resulted in resonance effects, enhancing the magnitude of beta oscillations.

II. Methods

The structure of the closed loop cortico-basal ganglia model developed in this study is presented in Fig. 1. The model is based on an extension of the basal ganglia network model originally presented by Rubin and Terman [27], [28]. In addition to the indirect pathway from the GPe through the STN to the GPi, the model also includes the hyperdirect pathway from the cortex to the STN and the pathway from the thalamus to cortex, thereby incorporating the closed loop formed by the cortex-STN-GPi and thalamus [34]. Striatal input to the GPe is implemented as a constant hyperpolarizing current. To incorporate STN plateau potentials, the model incorporates a more physiological representation of STN neurons introduced by Otsuka *et al.* [35]. It has been suggested that the generation of plateau potentials may be one of several mechanisms responsible for the long-lasting

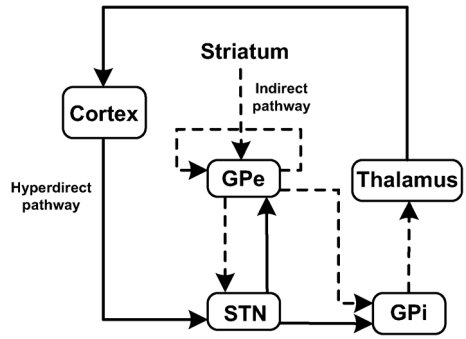

Fig. 1. Schematic diagram of the model, illustrating connections between GPe, STN, GPi, thalamus, striatum, and cortex. Excitatory connections are indicated with a solid line and inhibitory connections with a dashed line.

bursts observed in STN neurons [36] and that the ionic conductances underlying bursting activity in Parkinson's disease and plateau potentials may be the same [37]. Simulation of the GPe, GPi, and thalamus neurons was based on the neuron models presented in [27] and [28]. The GPe model was developed to match firing properties of GPe cells observed in slices. The GPi model is based on the GPe, with parameters altered to reflect faster firing properties of the GPi, while the thalamus is a simplification of a previously presented model [38].

It is assumed that the STN neurons receive substantial direct excitatory input from the cortex [39] via the hyperdirect pathway and inhibitory input from the GPe [40]. To represent these connections, each STN neuron in the model, receives excitatory input from two cortical neurons and inhibitory input from two GPe neurons. To simulate inhibitory connections between GPe neurons [41], each GPe neuron receives inhibitory input from two other GPe neurons in addition to excitatory input from a single STN neuron as the GPe is reciprocally connected to the STN [42]. Each GPi neuron receives excitatory input from a single STN neuron and inhibitory input from a single GPe neuron [43]. Finally, each thalamic neuron receives inhibitory input from a single GPi neuron and projects to the cortex such that each cortical neuron receives excitatory input from a single thalamic neuron (Fig. 1). As the details of connections between thalamic and cortical neurons are not well understood, in the model a simple one-to-one connectivity scheme was implemented. The effect of the striatum on the GPe was incorporated by applying a constant inhibitory current from the striatum to all GPe neurons. 25 STN, 25 GPe, 25 GPi, 10 thalamic neurons, and 25 cortical neurons were included in the model.

A. Subthalamic Nucleus Neurons

The STN model adopted here is that developed by Otsuka *et al.* (2004) as it captures critical STN properties in particular the generation of plateau potentials in a single compartment model, thereby remaining computationally efficient and suitable for including in a network model comprised of a large number of neurons. The membrane potential of STN neuron i, $v_{m_{\mathrm{STN}_i}}$ is described by

$$C_{m_{\mathrm{STN}_i}}\frac{dv_{m_{\mathrm{STN}_i}}}{dt} = -I_{Na_{\mathrm{STN}_i}} - I_{K_{\mathrm{STN}_i}} - I_{A_{\mathrm{STN}_i}} - I_{L_{\mathrm{STN}_i}} - I_{T_{\mathrm{STN}_i}} - I_{Ca-K_{\mathrm{STN}_i}} - I_{l_{\mathrm{STN}_i}} - I_{\alpha_i\to\beta_i} + I_{\mathrm{app}_{\mathrm{STN}}} \quad (1)$$

where $C_{m_{\mathrm{STN}_i}}$ is the membrane capacitance, $I_{Na_{\mathrm{STN}_i}}$ is the sodium current, $I_{K_{\mathrm{STN}_i}}$ is the Kv3-type K^+ current, and $I_{A_{\mathrm{STN}_i}}$ is the voltage dependent A-type K^+ current. An L-like long-lasting Ca^{2+} current, $I_{L_{\mathrm{STN}_i}}$, and low threshold T-type Ca^{2+} current, $I_{T_{\mathrm{STN}_i}}$ are also included. Finally, the model includes a Ca^{2+}-activated K^+ current, $I_{Ca-K_{\mathrm{STN}_i}}$, and a leak current, $I_{l_{\mathrm{STN}_i}}$. Parameter values used for the STN neuron are as detailed in Otsuka *et al.* (2004). $I_{\mathrm{app}_{\mathrm{STN}}}$ represents a level of activation of postsynaptic dopamine receptors in the STN. $I_{\alpha_i\to\beta_i}$ represents the synaptic current from cell α_i to cell β_i and is described as follows:

$$I_{\alpha_i\to\beta_i} = g_{\alpha_i\to\beta_i}\left(v_{\beta_i} - v_{\alpha_i\to\beta_i}\right)\sum_{j=1}^{n} s_j \tag{2}$$

where $g_{\alpha_i\to\beta_i}$ indicates the synaptic gain from structure α_i to structure β_i and $v_{\alpha_i\to\beta_i}$ is the reversal potential of the synaptic current. The sum is taken over the presynaptic neurons connected to each neuron. Details of the parameter values for the synaptic variable, s_j are given in Rubin and Terman (2004).

B. Globus Pallidus Neurons

The models used to simulate the GPe and GPi neurons are adopted from those presented in Rubin and Terman (2004). Similar to the equation for the STN neurons, the membrane potential of GPe neuron i, $v_{m_{\mathrm{GPe}_i}}$ is described by

$$\begin{aligned} C_{m_{\mathrm{GPe}_i}}\frac{dv_{m_{\mathrm{GPe}_i}}}{dt} &= -I_{L_{\mathrm{GPe}_i}} - I_{K_{\mathrm{GPe}_i}} - I_{Na_{\mathrm{GPe}_i}} - I_{T_{\mathrm{GPe}_i}} \\ &\quad -I_{Ca_{\mathrm{GPe}_i}} - I_{AHP_{\mathrm{GPe}_i}} - I_{\alpha_i\to\beta_i} + I_{\mathrm{app}_{GP}} + I_{N_i}. \end{aligned} \tag{3}$$

Here, $C_{m_{\mathrm{GPe}_i}}, I_{L_{\mathrm{GPe}_i}}, I_{K_{\mathrm{GPe}_i}}, I_{Na_{\mathrm{GPe}_i}}, I_{T_{\mathrm{GPe}_i}}, I_{Ca_{\mathrm{GPe}_i}}, I_{AHP_{\mathrm{GPe}_i}}$ indicate the membrane capacitance, leak, potassium, sodium, low-threshold T-type Ca^{2+}, high-threshold Ca^{2+}, and voltage-independent "afterhyperpolarization" K^+ currents, respectively. GPi neurons were modeled similarly to the GPe neurons. $I_{\alpha_i\to\beta_i}$ indicates the synaptic current as detailed in (2) and $I_{\mathrm{app}_{GP}}$ is a constant value representing the applied current from the striatum to the GPe in the GPe model and the additional constant current to the GPi to capture the neuron firing properties in the GPi model. I_{N_i} represents membrane noise added to the transmembrane potential of each GPe neuron. Details of the parameters for the GPe and GPi neurons and all additional constant current injected to each GPi neuron are presented in Rubin and Terman (2004).

C. Thalamic Neurons

The thalamic neurons include four intrinsic currents as described in Rubin and Terman (2004); a leak current I_L, a sodium current I_{Na}, a potassium current I_K, a low-threshold calcium current I_T, and a GPi-thalamus interaction current $I_{\alpha_i\to\beta_i}$. The membrane voltage equation of the thalamic neuron i, $v_{m_{Th_i}}$ is of the form

$$C_{m_{Th_i}}\frac{dv_{Th_i}}{dt} = -I_{L_{Th_i}} - I_{Na_{Th_i}} - I_{K_{Th_i}} - I_{T_{Th_i}} - I_{\alpha_i\to\beta_i} \tag{4}$$

where $C_{m_{Th_i}}$ is 1 $\mathrm{pF}/\mu\mathrm{m}^2$ and $I_{\alpha_i\to\beta_i}$ for the synaptic current, (2).

D. Cortical Neurons

The primary role of the cortical neurons in the present study is to act as a source of excitatory input to the STN transmitted through the hyperdirect pathway, while receiving excitatory input from the thalamus. It should, therefore, exhibit fundamental properties of cortical neurons, while remaining computationally efficient. The model developed by Izhikevich [44] was, therefore, chosen as it exhibits key features of cortical neurons whilst remaining relatively simple and effective for computational simulation. The mathematical representation of cortical neuron i is given by a series of nonlinear ordinary differential equations of the form

$$\begin{aligned} \frac{dv_{\mathrm{cot}_i}}{dt} &= 0.04v_{\mathrm{cot}_i}^2 + 5v_{\mathrm{cot}_i} + 140 - u_i + I_{\alpha_i\to\beta_i} + I_{N_i} \\ \frac{du_i}{dt} &= a\left(bv_{\mathrm{cot}_i} - u_i\right) \end{aligned} \tag{5}$$

with the auxiliary after-spike resetting as follows:

$$\text{if } v_{\mathrm{cot}_i} \geq 30\ \mathrm{mV}, \text{then} \begin{cases} v_{\mathrm{cot}_i} & \to c \\ u_i & \to u_i + d \end{cases}. \tag{6}$$

Here, v_{cot_i} represents the membrane potential of cortical neuron i, and u_i represents a membrane recovery variable which accounts for the activation of K^+ ionic currents and inactivation of Na^+ ionic currents and provides negative feedback to v_i. The parameter a describes the time scale of the recovery variable u_i, when smaller values represent slower recovery. The parameter b describes the sensitivity of the recovery variable u to the subthreshold fluctuations of the membrane potential v_{cot_i}. I_{N_i} represents membrane noise added to the transmembrane potential of each cortical neuron. The constant c describes the after-spike reset value of the membrane potential caused by the fast high-threshold K^+ conductances and its typical value is -65 mV. Finally, the parameter d describes after-spike reset of the recovery variable u_i caused by slow high-threshold Na^+ and K^+ conductances.

Membrane noise was simulated as Gaussian white noise with mean of 0 and standard deviation of 0.0001 and 0.005 $\mu\mathrm{A}/\mathrm{cm}^2$ and was added to the membrane potential of each GPe and cortical neuron, respectively. This resulted in uncorrelated neural firing pattern under both normal and parkinsonian state.

E. DBS

DBS was implemented by adding an intracellular current to each STN neuron in the form of a series of periodic rectangular current pulses, I_{DBS} of variable amplitude, duration, and frequency

$$\begin{aligned} C_{m_{\mathrm{STN}_i}}\frac{dv_{m_{\mathrm{STN}_i}}}{dt} &= -I_{Na_{\mathrm{STN}_i}} - I_{K_{\mathrm{STN}_i}} - I_{A_{\mathrm{STN}_i}} \\ &\quad -I_{L_{\mathrm{STN}_i}} - I_{T_{\mathrm{STN}_i}} - I_{Ca-K_{\mathrm{STN}_i}} - I_{l_{\mathrm{STN}_i}} - I_{\alpha_i\to\beta_i} \\ &\quad +I_{\mathrm{app}_{\mathrm{STN}}} + I_{\mathrm{DBS}}. \end{aligned} \tag{7}$$

F. Simulation Details

The synaptic gains to simulate normal conditions were initialized using values used in previous computational models [27], [28] and then adjusted so that the mean firing rates in each of the

TABLE I
MODEL PARAMETERS TO SIMULATE NORMAL AND DOPAMINE DEPLETED CONDITIONS

Parameter	Normal conditions	Dopamine depletion conditions
$g_{GPe\rightarrow STN}$	0.1	0.5
$g_{STN\rightarrow GPe}$	0.3	0.5
$g_{GPe\rightarrow GPe}$	1.0	2×10^{-2}
$g_{STN\rightarrow GPi}$	2×10^{-2}	0.1
$g_{GPe\rightarrow GPi}$	5×10^{-3}	5×10^{-3}
$g_{GPi\rightarrow Tha}$	5×10^{-2}	1.0
$g_{Tha\rightarrow Cot}$	4.0	7.0
I_{appSTN}	0.0	-1.5
I_{appGPe}	-0.2	-0.5
I_{appGPi}	-0.7	-1.2

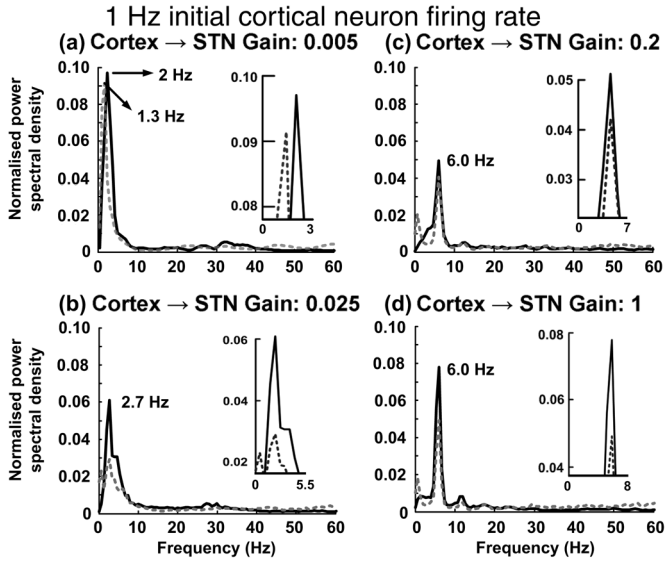

Fig. 2. Interaction of oscillations with initial frequencies of 1 Hz in the cortex and 1.3 Hz in the STN-GPe network. The average power spectrum of the cortical neurons is shown with a dashed line in gray and that of the STN neuron with a solid line in black. For low synaptic gains between the cortex and STN, the power spectra of the neurons in the cortex and STN exhibit peak frequency components of 1.3 and 2 Hz, respectively (a). The two frequencies begin to converge on a single frequency of 2.7 Hz as the synaptic gain from the cortex to the STN is increased (b). As the gain is further increased, the frequency at which the oscillations converge increases to 6 Hz (c), with further increase in gain resulting in a strengthening of synchronous oscillations at that frequency (d). A segment of the axis on a smaller frequency scale is shown in the insert in each figure.

nuclei approximate experimentally observed *in vivo* firing statistics. The mean firing rates of the STN, GPe, and GPi model neurons were 7.5 ± 0.3, 19.9 ± 0.6, and 110 ± 15 Hz, respectively. These compare with mean firing rates observed during *in vivo* recordings of 8–11 Hz in STN neurons, 15–20 Hz in GPe neurons in awake, resting rats, and 60–100 Hz in GPi neurons in monkeys in the normal state [45]–[47].

To simulate parkinsonian conditions a hyperpolarizing current was first added to the GPe to elicit bursting of GPe neurons at approximately 5 Hz. Self-inhibition between GPe neurons was reduced and the gain from GPe to STN and from STN to GPe was increased resulting in synchronized bursting of the STN and GPe neurons at 1–2 Hz similar to the bursting activity observed in the isolated STN-GPe network *in vitro* by Plenz and Kital (1999). The other synaptic gains in the closed loop cortex-STN-GPi-thalamus-cortex network were then also increased, consistent with the theory that dopamine has an overall damping effect on the network and that dopamine depletion leads to increased network excitability and synchronization [48]. Previous computational models have similarly increased connection strength between nuclei to simulate the effects of dopamine depletion on basal ganglia network activity in Parkinson's disease [32], [49], [50]. The synaptic gains and external current to the STN, GPe, and GPi are presented in Table I. The strength of the synaptic gain from the cortex to STN was then progressively increased from 0.0001 to 20 and the effect on the power spectra of the cortical and STN neurons was examined for initial cortical firing rates of 1, 10, 20, 30, 50, and 90 Hz.

The gain from cortex to STN and cortical neuron firing rates necessary to elicit synchronous oscillations within the entire network at the frequency of both parkinsonian tremor (4 Hz) and beta activities (20 Hz) were then identified and the effect of the DBS added directly to the STN neurons was considered under both conditions. The strength of tremor or beta oscillations in the average power spectra of the STN neurons was examined as the frequency of the DBS was progressively increased for DBS amplitudes of 130 and 200 $\mu\mathrm{A}/\mathrm{cm}^2$, respectively, and a pulse duration of 100 μs.

Simulations were performed using XPPAUT [51]. An adaptive-step fourth order Runge-Kutta method was used to solve the differential equations with a time step of 0.01 ms. To obtain a quantitative measure for the effect of the DBS on the cortico-basal ganglia network, each condition was simulated for a duration of 10 s in three separate simulation experiments, the power of the membrane potential of the STN and cortical neurons in the frequency band of interest was examined and the mean and standard deviation over all results evaluated. User developed programs using Welch's method in Matlab (Mathworks, Natick, MA, USA) were used to calculate total power spectral density of the membrane potentials across all neurons in the STN to quantify the magnitude of the tremor and beta band oscillations.

III. RESULTS

A. Interaction of Oscillations

Under simulated dopamine depletion conditions, the reciprocally connected STN-GPe network exhibited oscillatory bursting of both GPe and STN neurons at a frequency of 1.3 Hz, with a firing frequency of approximately 60 Hz within bursts. Inhibitory input from the GPe to the STN elicited rebound bursting of STN neurons, which in turn resulted in excitation of GPe neurons thus inhibiting the STN again. The power spectra of the STN and cortical neurons were then compared as the gain between cortex and STN, and the firing rate of the cortical neurons were systematically increased.

In Fig. 2, the average power spectra of all STN and cortical neurons are compared for increasing values of the gain between the cortex and STN, for an initial cortical firing rate of 1 Hz. The power spectra are compared as the gain was increased for

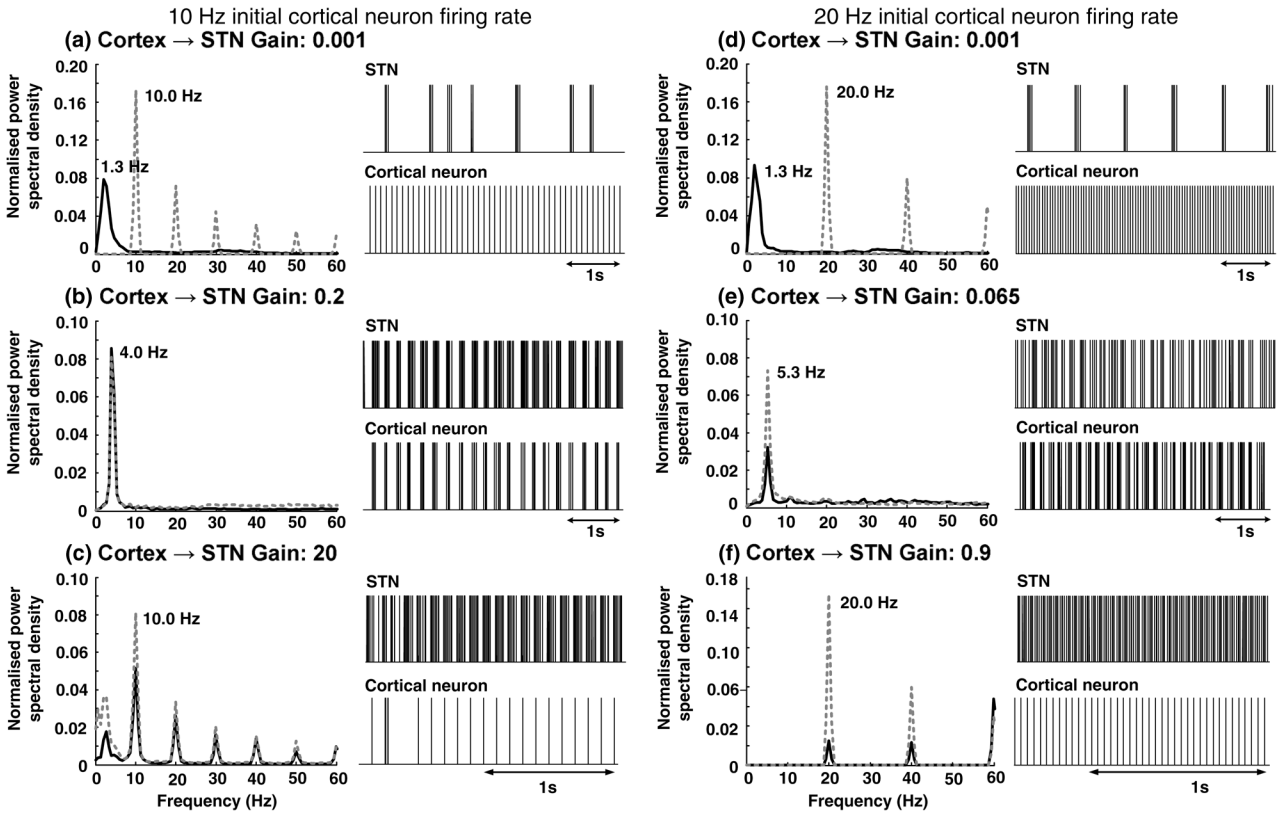

Fig. 3. Interaction of oscillations with initial frequencies of 10 Hz (a)–(c) and 20 Hz (d)–(f) in the cortex and 1.3 Hz in STN-GPe network. The average power spectra of the cortical neuron is shown with a dashed line in gray and that of the STN neuron with a solid line in black. For low synaptic gain between the cortex and STN, the power spectra of the neurons in the cortex and STN exhibit peak frequency components of 10 Hz or 20 Hz and 1.3 Hz, respectively (a), (d). As the synaptic gain is increased, the cortical and STN neurons begin to converge on a single frequency of 4.0 Hz for an initial cortical firing rate of 10 Hz (b) and 5.3 Hz for an initial cortical firing rate of 20 Hz (e). When the strength of the coupling between the cortex and the STN is increased further, the STN and GPe network is driven at the frequency of the cortical neuron firing (c), (f). Pulse trains representing the firing times of a representative STN and cortical neuron are shown in each figure.

TABLE II
PEAK FREQUENCIES OF POWER SPECTRA OF STN AND CORTEX AS THE GAIN AND INITIAL CORTICAL FIRING FREQUENCY WERE VARIED

	Initial cortical firing frequencies					
	30 Hz		50 Hz		90 Hz	
	Peak frequencies of power spectra (Hz)					
Cortex-STN gain	STN	Cortex	STN	Cortex	STN	Cortex
0.001	1.3	30.0	1.3	50.0	1.3	90
0.020	7.3	7.3	8.7	8.7	4.7	88.7
0.060	32.0	6.7	50.0	50.0	90.0	90.0
0.100	30.0	30.0	50.0	50.0	90.0	90.0

initial cortical firing rates of 10 and 20 Hz in Fig. 3. Each power spectrum has been normalized with respect to the total power. Peak frequencies in the STN and cortical neuron power spectra are presented in Table II for initial cortical firing rates of 30, 50, and 90 Hz.

For low gains between the cortex and STN, the STN-GPe network and cortical neurons were effectively uncoupled and exhibited oscillatory activity at distinct frequencies, with a peak in the power spectrum of the STN neurons at 1.3 Hz and in the cortical neurons at the frequency of cortical firing (Fig. 3(a) and (d), and Table II). As the gain from the cortex to the STN was increased, the cortical firing rate and the frequency of the STN-GPe oscillatory activity converged upon a new single intermediate frequency of synchronization throughout the network (Fig. 2(b)–(d), Fig. 3(b) and (e), and Table II). For initial cortical firing rates of 1, 10, 20, 30, and 50 Hz the peak in the power spectrum of the transmembrane potential of all neurons within the cortico-basal ganglia network converged on a frequency of 6.0, 4.0, 5.3, 7.3, and 8.7 Hz, respectively (Fig. 2(d), Fig. 3(b) and (e), and Table II). The emergence of a single dominant frequency throughout the network occurred at progressively lower gains as the cortical firing rate increased. The peaks in the power spectra of the cortical and STN neurons converged upon a single frequency at cortex-STN gains of 1.00, 0.20, 0.065, 0.02, and 0.02, for cortical firing rates of 1, 10, 20, 30, and 50 Hz, respectively. At the highest cortical firing rate examined, 90 Hz, the majority of cortical power remained at 90 Hz as the cortex-STN gain increased and convergence of the network on a lower frequency was not observed, Table II.

When the gain between the cortex and STN was further increased, a strong input from the cortex caused the STN neurons to be "driven" by the cortex at the same frequency as the cortical neurons. For cortical firing rates of 10, 20, 30, 50, and 90 Hz, bursting of STN neurons was driven at the frequency of the cortical input to the STN when the strength of the gain between the

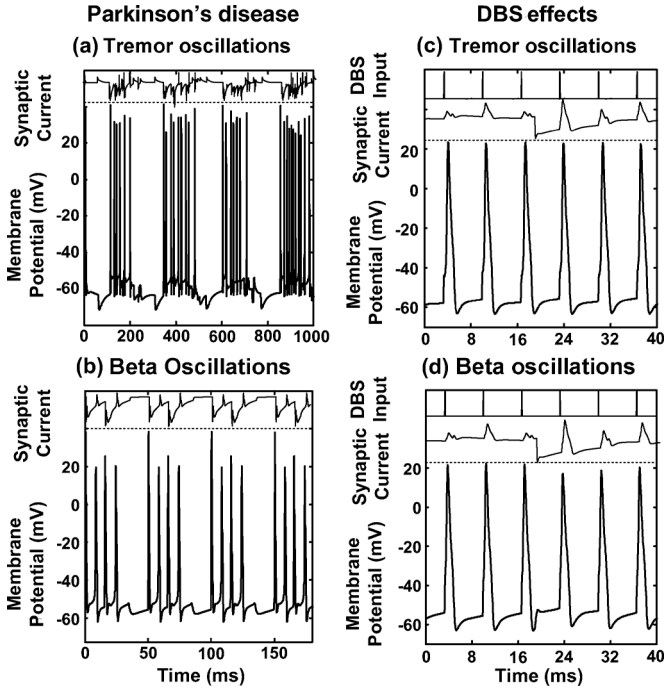

Fig. 4. Representative STN neuron oscillating at the tremor (a) and beta frequencies (b) and with DBS (c), (d). Total synaptic currents to the STN neuron from the cortex and GPe are shown on the top of each figure and the DBS input stimulus to the STN is also presented in (c) and (d).

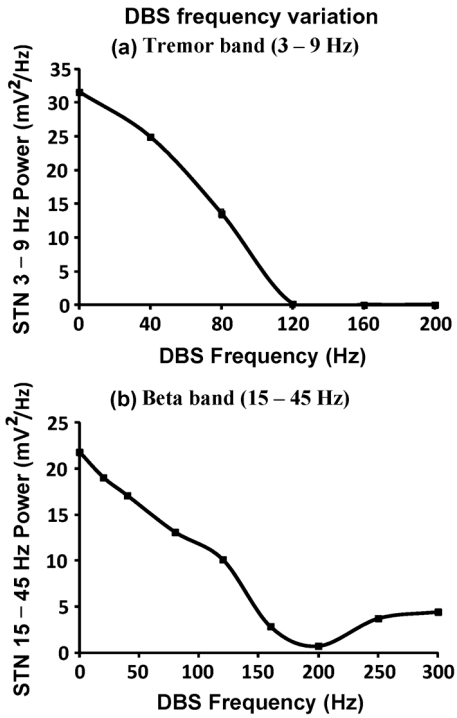

Fig. 5. Effect of DBS frequency on (a) the 3–9 Hz power of the membrane potential of a representative STN neuron and (b) the 15–45 Hz power as the frequency of the DBS stimulus was increased in the model of tremor and beta frequency oscillations, respectively. Data shows the mean ± standard deviation of three simulations of duration 10 s each. The DBS pulse duration was 100 μs in each case (a) and (b). The amplitude of 130 $\mu\mathrm{A/cm}^2$ was used in (a) and 200 $\mu\mathrm{A/cm}^2$ for (b).

cortex and STN was increased beyond the value at which convergence and loss of segregation throughout the network were initially observed (Fig. 3(c) and (f) and Table II). For the highest frequencies of cortical firing examined, 30, 50, and 90 Hz, the STN neurons were readily driven by the cortical input at relatively low levels of synaptic gains (Table II). In contrast, for the lowest value of cortical firing rate examined, 1 Hz, the network converged on a higher frequency of 6 Hz and driving of the network at the initial cortical firing frequency was not observed for the gains examined (Fig. 2). The oscillatory activity and neural firing patterns observed in the GPe were similar those in the STN.

B. Effect of DBS

To examine the effect of DBS in suppressing simulated oscillations at the frequency of parkinsonian tremor within the network, a cortical firing rate of 10 Hz and cortex-STN gain of 0.2 was chosen to generate oscillations throughout the network at 4.0 Hz [Fig. 3(b)]. A cortical firing rate of 20 Hz and cortex-STN gain of 0.9 [Fig. 3(f)] was chosen to generate oscillations at 20 Hz to examine the effect of DBS on simulated beta activity. Regular and synchronous bursting activity at 4 and 20 Hz, respectively, was observed in the STN [Fig. 4(a) and (b)].

The STN neurons were driven by the stimulation current and pathological oscillations were abolished with 150 Hz DBS with a pulse duration of 100 μs and 130 $\mu\mathrm{A/cm}^2$ amplitude for tremor frequency oscillations and 200 $\mu\mathrm{A/cm}^2$ amplitude for beta frequency oscillations [Fig. 4(c) and (d)]. The effect of varying the frequency of DBS on tremor and beta frequency oscillations was then examined for DBS amplitudes of 130 and 200 $\mu\mathrm{A/cm}^2$, respectively, and pulse duration of 100 μs. The power in the 3–9 Hz range of the membrane potential of a representative STN neuron in the tremor model is shown as the frequency of the DBS stimulus was increased [Fig. 5(a)]. Similarly, the power in the 15–45 Hz range for DBS applied to the model of beta oscillations is shown in Fig. 5(b). The total power at the frequency of the simulated pathological oscillations decreased as the frequency of the DBS stimulus was increased. A slight tendency for beta band activity to increase again as the DBS frequency increased above approximately 200 Hz was observed.

To allow comparison with experimental results in which low frequency DBS was applied to the STN, the change in 15–45 Hz STN power for DBS at 5, 10, and 20 Hz was compared to the beta band power without DBS, Fig. 6. Two conditions with different baseline levels of beta band activity were considered by varying the gain to the STN neurons from the cortex. For the lower baseline levels of beta activity, an increase in beta band activity was observed when DBS was applied at 5, 10, and 20 Hz while a small decrease was shown under the condition with higher baseline levels of beta activity. In both cases a decrease in the beta band power to 1.35 and 2.85 $\mathrm{mV}^2/\mathrm{Hz}$ was observed for DBS at 160 Hz.

IV. Discussion

A new computational model of the cortico-basal ganglia network has been presented. The model was used to explore the interaction of neural oscillations at different frequencies within the cortico-basal ganglia loop as the gain between the cortex

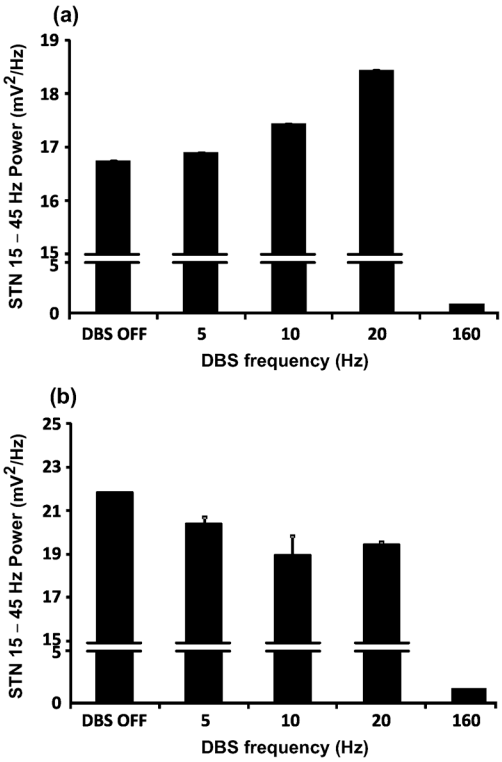

Fig. 6. Effect of low-frequency DBS on the 15–45 Hz power of a representative STN neuron. Two different baseline levels of the beta band activity were considered (a) low beta activity and (b) high beta activity under conditions of no DBS applied to the STN.

and STN was enhanced. By incorporating a closed loop cortico-basal ganglia network and the generation of oscillatory activity at both tremor and beta frequencies, the model provides a more comprehensive model in which to examine the effect of DBS parameters on pathological oscillations, than previous models which have considered either tremor generation [28]–[31] or beta oscillations [32], [33]. In addition, the model provides a framework for examining the effects of DBS parameters on the propagation of low frequency oscillatory activity throughout the cortico-basal ganglia network.

A. Generation and Interaction of Synchronous Oscillations within the Cortico-Basal Ganglia Network under Simulated Dopamine Depletion

The present study has focused on the generation of synchronous oscillations as a result of increased coupling between the cortex and STN through the fast hyperdirect pathway. Electrophysiological [20], [21], [23], [24] and recent imaging studies [22] have provided strong evidence of increased functional connectivity between the cortex and STN. These studies suggest a critical role for overactivity in the hyperdirect pathway in the generation of pathological synchronous activity, associated with akinesia and bradykinesia [10]–[12]. Consistent with this, the functional model proposed by Nambu *et al.*, suggests increased inhibition of expanded areas of the cortico-basal ganglia-thalamus network due to increased activity of the hyperdirect pathway in Parkinson's disease, suppressing the release of selected target motor programs [52].

At relatively low gains between the cortex and STN, the reciprocal connectivity between the STN and GPe network led to the generation of low-frequency (1.3 Hz) synchronous oscillatory activity within the simulated STN-GPe network. After the GPe neurons fired, inhibitory input to the STN resulted in rebound bursting of the STN, in turn leading to excitation of the GPe and the initiation of low-frequency oscillatory bursting in both nuclei. This effect was further facilitated by the reduction in self-inhibition between GPe neurons which increased the response of GPe neurons to excitatory inputs from the STN. The 1–2 Hz synchronized bursting observed in the STN-GPe network is similar to the synchronized oscillating bursts at 0.4–1.8 Hz in the isolated dopamine depleted STN-GPe network observed by Plenz and Kital (1999).

In the model, as the strength of the synaptic coupling from the cortex to STN was increased, low frequency, 1.3 Hz STN-GPe activity interacted with excitatory inputs from the cortex resulting in the emergence of synchronous oscillations throughout the network (STN, GPe, GPi, thalamus, and cortex) at a new intermediate frequency (Fig. 2(b)–(d), Fig. 3(b) and (e), and Table II). For cortical neurons firing at 10, 20, 30, and 50 Hz and low-frequency bursting of the STN-GPe network at 1.3 Hz, the network oscillations converged to a single frequency of 4.0, 5.3, 7.3, and 8.7 Hz, respectively. At high synaptic gains, a different mode of interaction was observed with periodic bursting of the STN driven at the frequency of the cortical neurons, synchronizing activity throughout the network (Fig. 3(c) and (f) and Table II).

The results are consistent with suggestions that increased synchronization and propagation of coherent beta band activity throughout the basal ganglia network may be due to enhanced sensitivity of the STN to beta activity originating in the cortex [20], [33], [53], [54]. The results presented here extend this hypothesis to illustrate how, for simulated dopamine depletion, oscillatory activity at the tremor and beta frequencies may arise either due to the interaction of oscillatory activity from two different sources, resulting in the emergence of synchronization throughout the network at a new frequency of oscillation, or when the gain is further increased, through driving of STN bursting by cortical inputs. Both result similarly in neural synchronization and a loss of segregation throughout the network (Figs. 2 and 3 and Table II). The model suggests a possible mechanism whereby oscillatory beta activity in the cortex interacting with slow oscillations in the STN-GPe network may lead to the emergence of oscillatory activity within the frequency range of parkinsonian tremor. As the sensitivity of the STN to cortical inputs is increased, the cortex may then drive the basal-ganglia network at frequencies in the beta range. Alternatively, it is also possible that beta activity may arise due to the interaction of low frequency activity with higher frequency activity originating in different neural populations.

Analysis of experimental data has suggested the presence of coupling and cross-frequency interactions between neural oscillations across different frequency bands. Nonlinear correlations between LFP oscillations at different frequencies have been reported in patients with Parkinson's disease, leading to a loss of segregation between rhythms [25]. Bispectral analysis has similarly indicated that low beta activity in the GPi generates

harmonics present in the high beta band and that these rhythms become independent following dopamine medication [26]. Increased LFP activity in the gamma frequency range was found to be associated with periods of stronger tremor in Parkinson's disease patients [55]. In addition, the ratio of beta to low gamma coherence was lower during these periods and higher during periods of weak tremor, leading to the suggestion that tremor is associated with an altered balance between beta and gamma activity [55]. The origin of the experimentally observed interactions between frequencies is unclear, however suggested possible mechanisms include synchronization between two or more oscillators comprised of populations of synchronized neurons [26], as observed in the model presented here.

Although the complexity of the model precludes the application of a theoretical analyses, the overall model behavior is similar to that predicted by simplified mean field models of interacting oscillations. The results are consistent with theoretical analyses of a simplified model of a closed-loop coupled network of neurons which predicts the interaction of two networks with different oscillation frequencies to produce a single frequency of oscillations lying between the two [56]. When the gains between two interacting networks are equal, the theoretical model predicts a new frequency of oscillations equal to the geometric mean of the two interacting frequencies, similar to that observed here (Fig. 3(b) and (e) and Table II).

B. Effect of DBS

The addition of high frequency stimulation from DBS directly affected the firing of STN neurons in this model, preventing the propagation of pathological oscillatory activity through the network (Fig. 4). Similar results were obtained when DBS was applied to either the GPi or thalamus, suggesting that the results are due to a cumulative network effect rather than targeting of a specific nucleus. This is similar to suggestions that DBS creates an "informational lesion" [57] or "jamming" [58] within the cortico-basal ganglia network. In terms of nonlinear control systems, the high frequency DBS input reduces the effective gain around the feedback loops involved, thus reducing unwanted lower frequency oscillations [59].

Tremor-frequency oscillations showed a continuous decrease with increasing DBS frequency, consistent with clinical recordings in essential tremor [60], with almost total suppression of the power occurring at and above approximately 120 Hz [Fig. 5(a)]. Similarly, the power of the STN membrane potential in the beta band was reduced as the DBS frequency increased. A continuous decrease in STN beta power was observed as the DBS frequency increased with a slight recovery at frequencies above 200 Hz [Fig. 5(b)].

In contrast to high frequency DBS low frequency stimulation of STN neurons has been shown to exacerbate parkinsonian symptoms. In recent studies, the effects of stimulation at low frequencies, including those in the beta band range were explored, based on baseline levels of tapping performance or the Unified Parkinson's Disease Rating Scale (UPDRS) [61]–[63]. To allow comparison with these results, two different baseline levels of beta activity were considered in the model when low frequency stimulation was applied to the STN. For the lower baseline levels, the beta power increased at low DBS frequencies of 5, 10, and 20 Hz due to resonance between the stimulus frequency and the network oscillations. In the case where relatively high baseline levels of beta band power were simulated, DBS at 5, 10, and 20 Hz resulted in a decrease in STN beta band activity as levels of beta activity in the network were already saturated prior to stimulation (Fig. 6). These simulation results are similar to the experimental results which showed the application of DBS at 5 and 20 Hz worsened performance when baseline tapping performance was within the normal range, but resulted in small increases in performance in subjects with baseline tapping function below the normal range [63]. Similar trends have been observed in UPDRS scores with STN DBS applied at 10 Hz [61].

C. Computational Model Limitations

The model is designed to capture critical pathways through the closed loop, cortex-STN-GPi-thalamus network. However, simplifying assumptions have necessarily been made. The model concentrated on the effects of the hyperdirect pathway and hence does not incorporate the striatal neurons or related projections, including the direct pathway. Inclusion of the direct pathway would reduce excitation within the GPi. Although it may modulate activity within the network, it would not be expected to alter the overall model behavior. Recent studies suggest an alternative possibility that enhanced beta frequency oscillations may arise from the interaction between medium spiny neuron GABAa current and intrinsic membrane currents within striatal networks [64]. Studies suggested that an intrinsic STN network, not considered in the present model, may also exist [65]. It is also likely that the thalamus may play a more complex role than a simple relay, as has been assumed [66]. The present study does not consider the volume conductor which determines voltage and current distribution in the tissue around electrode. Instead, the effect of DBS at the neuron is represented through the addition of an intracellular current, similar to the approach used in previous basal-ganglia network models of DBS [27]–[29], [31]. It has recently been suggested that DBS may be effective through simulation of afferent axons to the STN, rather than direct stimulation of the STN itself [67]. In this case, although the target would be different, the effects of DBS on low frequency neural oscillations would be expected to be similar to that observed here.

V. Conclusion

A model of the cortico-basal ganglia network has been presented to examine the interaction of oscillations at different frequencies within the network under conditions of dopamine depletion. The model was used to examine the effect of varying DBS frequency on oscillations within the tremor and beta bands. The results indicate that under conditions of enhanced sensitivity of STN neurons to cortical inputs, interaction of oscillatory activity within the STN-GPe network and cortex at different frequencies can result in the emergence of oscillatory activity at a new intermediate frequency. Under conditions of strong coupling between the cortex and STN, the cortex effectively drives the STN, leading to oscillatory activity throughout the network at the frequency of the cortical oscillations. When

DBS was added to the model, progressively increasing the DBS frequency reduced STN power within the frequency range of simulated tremor or beta oscillations, suppressing the propagation of oscillations through the network. Low frequency stimulation resulted in resonant effects which increased oscillations within the beta frequency range, consistent with previous experimental observations.

REFERENCES

[1] A. M. Lozano, J. Dostrovsky, R. Chen, and P. Ashby, "Deep brain stimulation for Parkinson's disease: Disrupting the disruption," *Lancet Neurol.*, vol. 1, no. 4, pp. 225–231, Aug. 2002.

[2] P. Brown, P. Mazzone, A. Oliviero, M. G. Altibrandi, F. Pilato, P. A. Tonali, and V. D. Lazzaro, "Effects of stimulation of the subthalamic area on oscillatory pallidal activity in Parkinson's disease," *Exp. Neurol.*, vol. 188, no. 2, pp. 480–490, Aug. 2004.

[3] H. Bergman, T. Wichmann, B. Karmon, and M. R. DeLong, "The primate subthalamic nucleus. II. Neuronal activity in the MPTP model of parkinsonism," *J. Neurophysiol.*, vol. 72, no. 2, pp. 507–520, Aug. 1994.

[4] J. M. Hurtado, C. M. Gray, L. B. Tamas, and K. A. Sigvardt, "Dynamics of tremor-related oscillations in the human globus pallidus: A single case study," *Proc. Nat. Acad. Sci. USA*, vol. 96, no. 4, pp. 1674–1679, Feb. 1999.

[5] R. Levy, W. D. Hutchison, A. M. Lozano, and J. O. Dostrovsky, "High-frequency synchronization of neuronal activity in the subthalamic nucleus of parkinsonian patients with limb tremor," *J. Neurosci.*, vol. 20, no. 20, pp. 7766–7775, Oct. 2000.

[6] J. F. Marsden, P. Limousin-Dowsey, P. Ashby, P. Pollak, and P. Brown, "Subthalamic nucleus, sensorimotor cortex and muscle interrelationships in Parkinson's disease," *Brain*, vol. 124, pt. 2, pp. 378–388, Feb. 2001.

[7] C. Reck, E. Florin, L. Wojtecki, H. Krause, S. Groiss, J. Voges, M. Maarouf, V. Sturm, A. Schnitzler, and L. Timmermann, "Characterisation of tremor-associated local field potentials in the subthalamic nucleus in Parkinson's disease," *Eur. J. Neurosci.*, vol. 29, no. 3, pp. 599–612, Feb. 2009.

[8] S.-Y. Wang, T. Z. Aziz, J. F. Stein, and X. Liu, "Time-frequency analysis of transient neuromuscular events: Dynamic changes in activity of the subthalamic nucleus and forearm muscles related to the intermittent resting tremor," *J. Neurosci. Methods*, vol. 145, no. 1–2, pp. 151–158, Jun. 2005.

[9] P. Tass, D. Smirnov, A. Karavaev, U. Barnikol, T. Barnikol, I. Adamchic, C. Hauptmann, N. Pawelcyzk, M. Maarouf, V. Sturm, H.-J. Freund, and B. Bezruchko, "The causal relationship between subcortical local field potential oscillations and parkinsonian resting tremor," *J. Neural Eng.*, vol. 7, no. 1, p. 16009, Feb. 2010.

[10] P. Brown and C. D. Marsden, "Bradykinesia and impairment of EEG desynchronization in Parkinson's disease," *Mov. Disord.*, vol. 14, no. 3, pp. 423–429, May 1999.

[11] A. A. Kühn, A. Kupsch, G.-H. Schneider, and P. Brown, "Reduction in subthalamic 8-35 Hz oscillatory activity correlates with clinical improvement in Parkinson's disease," *Eur. J. Neurosci.*, vol. 23, no. 7, pp. 1956–1960, Apr. 2006.

[12] A. A. Kühn, A. Tsui, T. Aziz, N. Ray, C. Brücke, A. Kupsch, G.-H. Schneider, and P. Brown, "Pathological synchronisation in the subthalamic nucleus of patients with Parkinson's disease relates to both bradykinesia and rigidity," *Exp. Neurol.*, vol. 215, no. 2, pp. 380–387, Feb. 2009.

[13] A. A. Kühn, F. Kempf, C. Brücke, L. Gaynor Doyle, I. Martinez-Torres, A. Pogosyan, T. Trottenberg, A. Kupsch, G.-H. Schneider, M. I. Hariz, W. Vandenberghe, B. Nuttin, and P. Brown, "High-frequency stimulation of the subthalamic nucleus suppresses oscillatory beta activity in patients with parkinson's disease in parallel with improvement in motor performance," *J. Neurosci.*, vol. 28, no. 24, pp. 6165–6173, Jun. 2008.

[14] H. Bronte-Stewart, C. Barberini, M. M. Koop, B. C. Hill, J. M. Henderson, and B. Wingeier, "The STN beta-band profile in Parkinson's disease is stationary and shows prolonged attenuation after deep brain stimulation," *Exp. Neurol.*, vol. 215, no. 1, pp. 20–28, Jan. 2009.

[15] A. Eusebio, W. Thevathasan, L. Doyle Gaynor, A. Pogosyan, E. Bye, T. Foltynie, L. Zrinzo, K. Ashkan, T. Aziz, and P. Brown, "Deep brain stimulation can suppress pathological synchronisation in parkinsonian patients," *J. Neurol. Neurosurg. Psychiatry*, vol. 82, no. 5, pp. 569–573, May 2011.

[16] D. Plenz and S. T. Kital, "A basal ganglia pacemaker formed by the subthalamic nucleus and external globus pallidus," *Nature*, vol. 400, no. 6745, pp. 677–682, Aug. 1999.

[17] J. Baufreton and M. D. Bevan, "D2-like dopamine receptor-mediated modulation of activity-dependent plasticity at GABAergic synapses in the subthalamic nucleus," *J. Physiol.*, vol. 586, no. 8, pp. 2121–2142, Apr. 2008.

[18] Z. Zhu, M. Bartol, K. Shen, and S. W. Johnson, "Excitatory effects of dopamine on subthalamic nucleus neurons: In vitro study of rats pretreated with 6-hydroxydopamine and levodopa," *Brain Res.*, vol. 945, no. 1, pp. 31–40, Jul. 2002.

[19] H. Bergman, A. Feingold, A. Nini, A. Raz, H. Slovin, M. Abeles, and E. Vaadia, "Physiological aspects of information processing in the basal ganglia of normal and parkinsonian primates," *Trends Neurosci.*, vol. 21, no. 1, pp. 32–38, Jan. 1998.

[20] P. J. Magill, J. P. Bolam, and M. D. Bevan, "Dopamine regulates the impact of the cerebral cortex on the subthalamic nucleus-globus pallidus network," *Neuroscience*, vol. 106, no. 2, pp. 313–330, 2001.

[21] E. Lalo, S. Thobois, A. Sharott, G. Polo, P. Mertens, A. Pogosyan, and P. Brown, "Patterns of bidirectional communication between cortex and basal ganglia during movement in patients with parkinson disease," *J. Neurosci.*, vol. 28, no. 12, pp. 3008–3016, Mar. 2008.

[22] S. Baudrexel, T. Witte, C. Seifried, F. von Wegner, F. Beissner, J. C. Klein, H. Steinmetz, R. Deichmann, J. Roeper, and R. Hilker, "Resting state fMRI reveals increased subthalamic nucleus-motor cortex connectivity in Parkinson's disease," *Neuroimage*, vol. 55, no. 4, pp. 1728–1738, Apr. 2011.

[23] D. Williams, M. Tijssen, G. V. Bruggen, A. Bosch, A. Insola, V. D. Lazzaro, P. Mazzone, A. Oliviero, A. Quartarone, H. Speelman, and P. Brown, "Dopamine-dependent changes in the functional connectivity between basal ganglia and cerebral cortex in humans," *Brain*, vol. 125, pt. 7, pp. 1558–1569, Jul. 2002.

[24] N. Mallet, A. Pogosyan, A. Sharott, J. Csicsvari, J. P. Bolam, P. Brown, and P. J. Magill, "Disrupted dopamine transmission and the emergence of exaggerated beta oscillations in subthalamic nucleus and cerebral cortex," *J. Neurosci.*, vol. 28, no. 18, pp. 4795–4806, Apr. 2008.

[25] S. Marceglia, G. Foffani, A. M. Bianchi, G. Baselli, F. Tamma, M. Egidi, and A. Priori, "Dopamine-dependent non-linear correlation between subthalamic rhythms in Parkinson's disease," *J. Physiol.*, vol. 571, pt. 3, pp. 579–591, Mar. 2006.

[26] S. Marceglia, A. M. Bianchi, G. Baselli, G. Foffani, F. Cogiamanian, N. Modugno, S. Mrakic-Sposta, A. Priori, and S. Cerutti, "Interaction between rhythms in the human basal ganglia: Application of bispectral analysis to local field potentials," *IEEE Trans. Neural Syst. Rehabil. Eng.*, vol. 15, no. 4, pp. 483–492, Dec. 2007.

[27] D. Terman, J. E. Rubin, A. C. Yew, and C. J. Wilson, "Activity patterns in a model for the subthalamopallidal network of the basal ganglia," *J. Neurosci.*, vol. 22, no. 7, pp. 2963–2976, Apr. 2002.

[28] J. E. Rubin and D. Terman, "High frequency stimulation of the subthalamic nucleus eliminates pathological thalamic rhythmicity in a computational model," *J. Comput. Neurosci.*, vol. 16, no. 3, pp. 211–235, 2004.

[29] X.-J. Feng, E. Shea-Brown, B. Greenwald, R. Kosut, and H. Rabitz, "Optimal deep brain stimulation of the subthalamic nucleus-a computational study," *J. Comput. Neurosci.*, vol. 23, no. 3, pp. 265–282, Dec. 2007.

[30] C. Hauptmann, O. Popovych, and P. A. Tass, "Desynchronizing the abnormally synchronized neural activity in the subthalamic nucleus: A modeling study," *Expert Rev. Med. Devices*, vol. 4, no. 5, pp. 633–650, Sep. 2007.

[31] M. Pirini, L. Rocchi, M. Sensi, and L. Chiari, "A computational modelling approach to investigate different targets in deep brain stimulation for Parkinson's disease," *J. Comput. Neurosci.*, vol. 26, no. 1, pp. 91–107, Feb. 2009.

[32] P. J. Hahn and C. C. McIntyre, "Modeling shifts in the rate and pattern of subthalamopallidal network activity during deep brain stimulation," *J. Comput. Neurosci.*, vol. 28, no. 3, pp. 425–441, Jun. 2010.

[33] R. Moran, N. Mallet, V. Litvak, R. Dolan, P. Magill, K. Friston, and P. Brown, "Alterations in brain connectivity underlying beta oscillations in parkinsonism," *PLoS Comput. Biol.*, vol. 7, p. e1002124, Aug. 2011.

[34] A. Parent and L. N. Hazrati, "Functional anatomy of the basal ganglia. I. The cortico-basal ganglia-thalamo-cortical loop," *Brain Res. Brain Res. Rev.*, vol. 20, no. 1, pp. 91–127, Jan. 1995.

[35] T. Otsuka, T. Abe, T. Tsukagawa, and W.-J. Song, "Conductance-based model of the voltage-dependent generation of a plateau potential in subthalamic neurons," *J. Neurophysiol.*, vol. 92, no. 1, pp. 255–264, Jul. 2004.

[36] T. Otsuka, F. Murakami, and W. J. Song, "Excitatory postsynaptic potentials trigger a plateau potential in rat subthalamic neurons at hyperpolarized states," *J. Neurophysiol.*, vol. 86, no. 4, pp. 1816–1825, Oct. 2001.
[37] C. Beurrier, P. Congar, B. Bioulac, and C. Hammond, "Subthalamic nucleus neurons switch from single-spike activity to burst-firing mode," *J. Neurosci.*, vol. 19, no. 2, pp. 599–609, Jan. 1999.
[38] V. S. Sohal and J. R. Huguenard, "Reciprocal inhibition controls the oscillatory state in thalamic networks," *Neurocomp*, vol. 44, pp. 653–659, 2002.
[39] R. L. Albin, A. B. Young, and J. B. Penney, "The functional anatomy of basal ganglia disorders," *Trends Neurosci.*, vol. 12, no. 10, pp. 366–375, Oct. 1989.
[40] K. Fujimoto and H. Kita, "Response characteristics of subthalamic neurons to the stimulation of the sensorimotor cortex in the rat," *Brain Res.*, vol. 609, no. 1–2, pp. 185–192, Apr. 1993.
[41] H. Kita and S. T. Kitai, "The morphology of globus pallidus projection neurons in the rat: An intracellular staining study," *Brain Res.*, vol. 636, no. 2, pp. 308–319, Feb. 1994.
[42] H. Nakanishi, H. Kita, and S. T. Kitai, "Intracellular study of rat substantia nigra pars reticulata neurons in an in vitro slice preparation: Electrical membrane properties and response characteristics to subthalamic stimulation," *Brain Res.*, vol. 437, no. 1, pp. 45–55, Dec. 1987.
[43] Y. Smith, L. N. Hazrati, and A. Parent, "Efferent projections of the subthalamic nucleus in the squirrel monkey as studied by the pha-l anterograde tracing method," *J. Comp. Neurol.*, vol. 294, no. 2, pp. 306–323, Apr. 1990.
[44] E. M. Izhikevich, "Simple model of spiking neurons," *IEEE Trans. Neural Netw.*, vol. 14, no. 6, pp. 1569–1572, Nov. 2003.
[45] T. Boraud, E. Bezard, B. Bioulac, and C. Gross, "High frequency stimulation of the internal Globus Pallidus (GPi) simultaneously improves parkinsonian symptoms and reduces the firing frequency of GPi neurons in the MPTP-treated monkey," *Neurosci. Lett.*, vol. 215, no. 1, pp. 17–20, Aug. 1996.
[46] D. S. Kreiss, C. W. Mastropietro, S. S. Rawji, and J. R. Walters, "The response of subthalamic nucleus neurons to dopamine receptor stimulation in a rodent model of Parkinson's disease," *J. Neurosci.*, vol. 17, no. 17, pp. 6807–6819, Sep. 1997.
[47] N. Urbain, D. Gervasoni, F. Soulière, L. Lobo, N. Rentéro, F. Windels, B. Astier, M. Savasta, P. Fort, B. Renaud, P. H. Luppi, and G. Chouvet, "Unrelated course of subthalamic nucleus and globus pallidus neuronal activities across vigilance states in the rat," *Eur. J. Neurosci.*, vol. 12, no. 9, pp. 3361–3374, Sep. 2000.
[48] A. V. Cruz, N. Mallet, P. J. Magill, P. Brown, and B. B. Averbeck, "Effects of dopamine depletion on network entropy in the external globus pallidus," *J. Neurophysiol.*, vol. 102, no. 2, pp. 1092–1102, Aug. 2009.
[49] M. D. Humphries, R. D. Stewart, and K. N. Gurney, "A physiologically plausible model of action selection and oscillatory activity in the basal ganglia," *J. Neurosci.*, vol. 26, no. 50, pp. 12 921–12 942, Dec. 2006.
[50] A. Moran, E. Stein, H. Tischler, K. Belelovsky, and I. Bar-Gad, "Dynamic stereotypic responses of basal ganglia neurons to subthalamic nucleus high-frequency stimulation in the parkinsonian primate," *Front. Syst. Neurosci.*, vol. 5, p. 21, 2011.
[51] B. Ermentrout, *Simulating, Analyzing, and Animating Dynamical Systems*. Philadelphia, PA: SIAM, 2002.
[52] A. Nambu, "A new approach to understand the pathophysiology of Parkinson's disease," *J. Neurol.*, vol. 252, pp. IV1–IV4, Oct. 2005.
[53] R. Levy, P. Ashby, W. D. Hutchison, A. E. Lang, A. M. Lozano, and J. O. Dostrovsky, "Dependence of subthalamic nucleus oscillations on movement and dopamine in Parkinson's disease," *Brain*, vol. 125, pt. 6, pp. 1196–1209, Jun. 2002.
[54] P. Brown, "Abnormal oscillatory synchronisation in the motor system leads to impaired movement," *Curr. Opin. Neurobiol.*, vol. 17, no. 6, pp. 656–664, Dec. 2007.
[55] M. Weinberger, W. D. Hutchison, A. M. Lozano, M. Hodaie, and J. O. Dostrovsky, "Increased gamma oscillatory activity in the subthalamic nucleus during tremor in Parkinson's disease patients," *J. Neurophysiol.*, vol. 101, no. 2, pp. 789–802, Feb. 2009.
[56] A. M. de Paor and M. M. Lowery, "Can control theory throw light on parkinson's disease and its treatment with deep brain stimulation?," in *IET Irish Signals Syst. Conf. (ISSC2009)*, 2009, pp. 1–6.
[57] W. M. Grill, A. N. Snyder, and S. Miocinovic, "Deep brain stimulation creates an informational lesion of the stimulated nucleus," *Neuroreport*, vol. 15, no. 7, pp. 1137–1140, May 2004.
[58] A. L. Benabid, A. Benazzouz, and P. Pollak, "Mechanisms of deep brain stimulation," *Mov. Disord.*, vol. 17, pp. S73–S74, 2002.
[59] A. M. de Paor and M. M. Lowery, "Analysis of the mechanism of action of deep brain stimulation using the concepts of dither injection and the equivalent nonlinearity," *IEEE Trans. Biomed. Eng.*, vol. 56, no. 11, pt. 2, pp. 2717–2720, Nov. 2009.
[60] M. Ushe, J. W. Mink, S. D. Tabbal, M. Hong, P. S. Gibson, K. M. Rich, K. E. Lyons, R. Pahwa, and J. S. Perlmutter, "Postural tremor suppression is dependent on thalamic stimulation frequency," *Mov. Disord.*, vol. 21, no. 8, pp. 1290–1292, Aug. 2006.
[61] L. Timmermann, L. Wojtecki, J. Gross, R. Lehrke, J. Voges, M. Maarouf, H. Treuer, V. Sturm, and A. Schnitzler, "Ten-Hertz stimulation of subthalamic nucleus deteriorates motor symptoms in Parkinson's disease," *Mov. Disord.*, vol. 19, no. 11, pp. 1328–1333, Nov. 2004.
[62] C. C. Chen, V. Litvak, T. Gilbertson, A. Kühn, C. S. Lu, S. T. Lee, C. H. Tsai, S. Tisch, P. Limousin, M. Hariz, and P. Brown, "Excessive synchronization of basal ganglia neurons at 20 Hz slows movement in Parkinson's disease," *Exp. Neurol.*, vol. 205, no. 1, pp. 214–221, May 2007.
[63] A. Eusebio, C. C. Chen, C. S. Lu, S. T. Lee, C. H. Tsai, P. Limousin, M. Hariz, and P. Brown, "Effects of low-frequency stimulation of the subthalamic nucleus on movement in Parkinson's disease," *Exp. Neurol.*, vol. 209, no. 1, pp. 125–130, Jan. 2008.
[64] M. M. McCarthy, C. Moore-Kochlacs, X. Gu, E. S. Boyden, X. Han, and N. Kopell, "Striatal origin of the pathologic beta oscillations in Parkinson's disease," *Proc. Nat. Acad. Sci. USA*, vol. 108, no. 28, pp. 11 620–11 625, Jul. 2011.
[65] R. Ammari, C. Lopez, B. Bioulac, L. Garcia, and C. Hammond, "Subthalamic nucleus evokes similar long lasting glutamatergic excitations in pallidal, entopeduncular and nigral neurons in the basal ganglia slice," *Neuroscience*, vol. 166, no. 3, pp. 808–818, Mar. 2010.
[66] M. Castle, M. S. Aymerich, C. Sanchez-Escobar, N. Gonzalo, J. A. Obeso, and J. L. Lanciego, "Thalamic innervation of the direct and indirect basal ganglia pathways in the rat: Ipsi- and contralateral projections," *J. Comp. Neurol.*, vol. 483, no. 2, pp. 143–153, Mar. 2005.
[67] V. Gradinaru, M. Mogri, K. R. Thompson, J. M. Henderson, and K. Deisseroth, "Optical deconstruction of parkinsonian neural circuitry," *Science*, vol. 324, no. 5925, pp. 354–359, Apr. 2009.

Guiyeom Kang received the B.E. degree in electronic engineering from the Waterford Institute of Technology, Waterford, Ireland, in 2006, and the M.E.Sc. degree in biomedical engineering, in 2010, from the University College Dublin, Dublin, Ireland, where she is currently working toward the Ph.D. degree with research interests in computational modeling of the basal ganglia and deep brain stimulation in Parkinson's disease.

Madeleine M. Lowery (M'12) received the B.E. and Ph.D. degrees from the Department of Electronic and Electrical Engineering, University College Dublin, Dublin, Ireland, in 1996 and 2000, respectively.

She is a Senior Lecturer in the School of Electrical, Electronic and Communications Engineering, University College Dublin. Her research involves the exploration of nerve and muscle activity through mathematical modeling, analysis, and experimentation, to increase understanding of neuromuscular activity in healthy and diseased states and develop novel and improved rehabilitation strategies. Her research interests include electromyography, myoelectric prosthetic control, bioelectromagnetics, electrical stimulation, deep brain stimulation and neural control of movement. Between 2000 and 2005, she was a Postdoctoral Fellow then Research Assistant Professor at the Rehabilitation Institute of Chicago and the Department of Physical Medicine and Rehabilitation, Northwestern University.

Dr. Lowery is a member of the Council of the International Society of Electrophysiology and Kinesiology (ISEK).